Impact of Sea-Ice Dynamics on the Spatial Distribution of Diatom Resting Stages in Sediments of the Pacific Arctic Region

Yuri Fukai[1,2] ⓘ, Kohei Matsuno[2,3] ⓘ, Amane Fujiwara[4] ⓘ, Koji Suzuki[1,5] ⓘ, Mindy L. Richlen[6], Evangeline Fachon[6], and Donald M. Anderson[6]

[1]Graduate School of Environmental Science, Hokkaido University, Sapporo, Japan, [2]Faculty/Graduate School of Fisheries Sciences, Hokkaido University, Hakodate, Japan, [3]Arctic Research Center, Hokkaido University, Sapporo, Japan, [4]Japan Agency for Marine-Earth Science and Technology, Yokosuka, Japan, [5]Faculty of Environmental Earth Science, Hokkaido University, Sapporo, Japan, [6]Biology Department, Woods Hole Oceanographic Institution, Woods Hole, MA, USA

Abstract The Pacific Arctic region is characterized by seasonal sea-ice, the spatial extent and duration of which varies considerably. In this region, diatoms are the dominant phytoplankton group during spring and summer. To facilitate survival during periods that are less favorable for growth, many diatom species produce resting stages that settle to the seafloor and can serve as a potential inoculum for subsequent blooms. Since diatom assemblage composition is closely related to sea-ice dynamics, detailed studies of biophysical interactions are fundamental to understanding the lower trophic levels of ecosystems in the Pacific Arctic. One way to explore this relationship is by comparing the distribution and abundance of diatom resting stages with patterns of sea-ice coverage. In this study, we quantified viable diatom resting stages in sediments collected during summer and autumn 2018 and explored their relationship to sea-ice extent during the previous winter and spring. Diatom assemblages were clearly dependent on the variable timing of the sea-ice retreat and accompanying light conditions. In areas where sea-ice retreated earlier, open-water species such as *Chaetoceros* spp. and *Thalassiosira* spp. were abundant. In contrast, proportional abundances of *Attheya* spp. and pennate diatom species that are commonly observed in sea-ice were higher in areas where diatoms experienced higher light levels and longer day length in/under the sea-ice. This study demonstrates that sea-ice dynamics are an important determinant of diatom species composition and distribution in the Pacific Arctic region.

Plain Language Summary The Pacific Arctic region is characterized by seasonal sea-ice, and there is considerable interannual variation in the timing and quality of ice presence. In this region, diatoms are the dominant phytoplankton group during spring and summer. Under conditions unfavorable for growth, such as low light or limiting nutrients, many diatom species produce resting stages that are similar to "seeds" of plants. These resting stages settle to the seafloor and can reflect the diatom assemblages in the overlying water column. Since diatom species distribution is closely related to sea-ice dynamics, detailed studies of this relationship are fundamental to understanding the basis of marine ecosystems in the Pacific Arctic region. In this study, we explored the relationship by comparing the distribution of diatom resting stage assemblages with patterns of sea-ice coverage. Diatom assemblages detected in sediments were dependent on the variable timing of the sea-ice retreat and accompanying light conditions. In areas where sea-ice retreated earlier, open-water species were abundant, while proportional abundances of ice-associated diatoms were higher in areas where diatoms experience favorable light conditions in/under the sea-ice. This study demonstrates that sea-ice dynamics are an important determinant of diatom composition in the Pacific Arctic region.

1. Introduction

The Pacific Arctic region extends from the northern Bering Sea to the Chukchi and Beaufort Seas. Within this region, the northern Bering and Chukchi Seas display among the highest daily rates of productivity in the world (Springer et al., 1996). Phytoplankton are responsible for high primary productivity in the euphotic layer and delivery of particulate organic carbon (POC) to the benthos. The sinking POC flux measured

in 2018 in the northern Bering and Chukchi Seas was the among highest ever documented across global oceans (O'Daly et al., 2020). This POC supports patchy distributions of high benthic biomass known as "benthic hotspots" (Grebmeier et al., 1988, 2006). In contrast, primary productivity in the southwestern Beaufort Sea is low (Frost & Lowry, 1984).

In the Arctic Ocean, ice algae production occurs in and under the sea ice, and is followed by phytoplankton blooms during the summer retreat of sea-ice (Horner, 1984; Horner & Schrader, 1982). Mean daily water column integrated primary productivity in the southwestern Beaufort Sea is about half of that of the Chukchi Sea, even during peak periods in June and July (Hill et al., 2018). Overall, annual primary production is much higher in the Chukchi shelf than on the Beaufort shelf (Grebmeier et al., 2006).

The Pacific Arctic region is characterized by the presence of seasonal sea-ice, which varies considerably in extent and duration from year to year. The extent of sea-ice has been shown to influence regional phytoplankton assemblages (Neeley et al., 2018), but this relationship is not fully understood. Sea-ice decline has been reported in the region (Frey et al., 2018; Grebmeier et al., 2015; Markus et al., 2009), and Arrigo et al. (2008) used satellite observations to show that this decline was associated with increasing annual primary production. However, changes in phytoplankton assemblages and particularly in ice-associated assemblages, cannot be evaluated by satellite observations only, necessitating field-based studies to examine the structure of these communities in more detail.

Phytoplankton assemblages during spring and summer blooms in the Pacific Arctic region are dominated by diatoms (von Quillfeldt, 2000; Sergeeva et al., 2010), which drive sinking POC flux (Lalande et al., 2020). Some diatom genera, *Chaetoceros* spp. and *Thalassiosira* spp., are known to form dense blooms in this region (von Quillfeldt, 2000; Sergeeva et al., 2010). In particular, *C. socialis s.l.* can constitute more than 90% of phytoplankton assemblages during blooms in the northern Bering and Chukchi Seas (Sergeeva et al., 2010). The centric diatoms *Attheya* spp. are reported to be present in the sea-ice of the Arctic (Campbell et al., 2018; Melnikov et al., 2002; von Quillfeldt et al., 2003; Szymanski & Gradinger, 2016; Werner et al., 2007) and can comprise over 60% of diatom abundance in the sea-ice during spring (Campbell et al., 2018). Pennate diatoms are also known to constitute a large proportion of the sea-ice algal community (von Quillfeldt et al., 2003; Szymanski & Gradinger, 2016).

Many diatom species form resting stages under unfavorable growth conditions such as nutrient limitation (Durbin, 1978; Garrison, 1984; McQuoid & Hobson, 1996; Smetacek, 1985), Fe limitation (Sugie & Kuma, 2008) and low light conditions (McQuoid & Hobson, 1996). High cell concentrations in water column assemblages can also induce formation of resting stages (Pelusi et al., 2020). Resting stages that sink to and accumulate in bottom sediments can germinate and resume growth in response to favorable light levels (Hollibaugh et al., 1981). The ability to form resting stages is thus an important life cycle strategy for survival under low temperature and light conditions during winter in seasonal sea-ice areas (Tsukazaki et al., 2013, 2018).

The distribution of diatom resting stage assemblages in sediments is thought to reflect the extent and magnitude of past blooms (Itakura et al., 1997; Pitcher, 1990) and can be used to investigate determinants of community structure and bloom dynamics. For example, in the northern Bering Sea, analysis of the diatom resting stages in sediments showed that diatom assemblages in early spring were dependent upon the timing of the sea-ice retreat (TSR): ice-associated diatoms were abundant in 2017 when the sea-ice remained until early April, but open-water diatoms dominated in 2018 when the TSR was approximately two weeks earlier than the previous year (Fukai et al., 2019).

In this study, we enumerated viable diatom resting stages in sediments collected in a broad area across the Pacific Arctic region, from the northern Bering Sea to the Chukchi Sea and the southwestern Beaufort Sea. We describe the features of diatom resting stage assemblages over these regions, and discuss two hypotheses: (a) the concentrations of diatom resting stage assemblages are correlated with primary production in the water column, and (b) the extent and duration of sea-ice during the previous winter and spring determines community structure of diatom resting stage assemblages. In addition, we discuss how observed variations in diatom assemblages may impact organisms at higher trophic levels that rely on diatoms as an important food source.
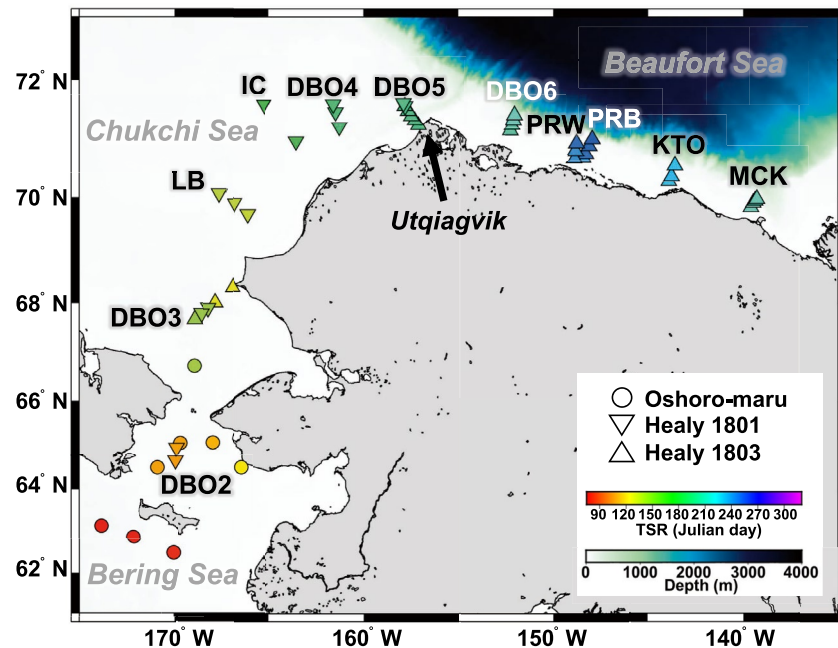
Figure 1. Sediment sampling locations in the northern Bering Sea, Chukchi Sea, and Beaufort Sea in 2018. Color contours indicate the timing of the sea-ice retreat (rainbow contour) and the bottom depth (blue contour). Abbreviations indicate the transect names during Healy cruises 1801 and 1803. SLI: St. Lawrence Island.

2. Materials and Methods

2.1. Sea-Ice, Primary Production and Daylight Hours

To evaluate the sea-ice extent in each region, the Advanced Microwave Scanning Radiometer 2 (AMSR2) standard sea-ice concentration (SIC) product was obtained from the Japan Aerospace Exploration Agency (JAXA) web portal (https://gportal.jaxa.jp/gpr/) at a 10-km resolution. The TSR was defined as the last day when the SIC fell below 20% prior to the observed annual sea-ice minimum across the study region during summer. Here, we used the SIC data after calculating a 5-day moving average.

To obtain a continuous primary production time-series, we used Level-3 standard mapped image (9-km resolution) of Aqua-MODIS data downloaded as spectral remote sensing reflectance (R_{rs}) and daily photosynthetically available radiation (PAR) from the Goddard Space Flight Centre/Distributed Active Archive Centre, NASA. The absorption coefficient for 443 nm ($a_{ph}(443)$) and euphotic zone depth (Z_{eu}) were computed from $R_{rs}(\lambda)$ using Quasi-Analytical Algorithm version 5 (Lee et al., 2007, 2009) and daylength (DL) for the study area calculated according to Brock (1981). We then computed the daily euphotic-depth-integrated primary production (PP_{eu}) using $a_{ph}(443)$, Z_{eu}, PAR, and DL as inputs to an absorption-based productivity model (ABPM (Hirawake et al., 2012)). Missing values in $a_{ph}(443)$ and Z_{eu} due to cloud cover were interpolated using their annual medians and hence PP_{eu} was derived for the cloud-covered pixels. From these values we calculated cumulative PP_{eu} (IP_{eu}) from TSR to the date of the in situ sediment sampling was conducted for each shipboard observation site.

2.2. Sampling

Sediment sampling was conducted in the shallow Pacific Arctic region at stations ranging from 24–194 m bottom depths (the northern Bering Sea, Chukchi Sea and the southwestern Beaufort Sea; Figure 1, Table 1) from July 2–12, 2018 aboard T/S *Oshoro-Maru* of Hokkaido University, and from August 9–23, 2018 and October 30 to November 15 2018 aboard the U.S. Coast Guard icebreaker Healy (HLY 1801 and HLY 1803, respectively) (Figure 2a). Sediment samples were collected using a multiple corer (*Oshoro-Maru* cruise), a Van Veen Grab sampler, or a HAPS core sampler (Healy cruises) at each station. A portion of the 0–1 cm of each sediment core was extruded and stored in darkness at 5°C for *Oshoro-Maru* samples, and for Healy

Table 1
Locations of Sediment Sampling Stations in the Bering, Chukchi, and Beaufort Seas From July to November in 2018

Cruise	Station	Date (Julian day)	Latitude (°N)	Longitude (°W)	Bottom depth (m)	Sample type	TSR (Julian day)	IP$_{eu}$ (mg C m^{-2})	GP (hours)
Oshoro-maru	OS4	2018/7/2 (183)	63.15	173.83	75	Core	2018/3/22 (81)	80,253.9	103.2
	OS6	2018/7/3 (184)	62.88	172.16	55	Core	2018/3/23 (82)	56,305.7	158.4
	OS8	2018/7/3 (184)	62.49	170.00	37	Core	2018/3/25 (84)	77,752.8	234.2
	OS14	2018/7/5 (186)	64.51	170.87	46	Core	2018/4/17 (107)	66,311.6	414.7
	OS19	2018/7/6 (187)	64.51	166.51	28	Core	2018/5/1 (121)	39,181.0	755.1
	OS20	2018/7/6 (187)	65.08	168.00	46	Core	2018/4/20 (110)	32,002.1	581.4
	OS22	2018/7/7 (188)	65.07	169.70	51	Core	2018/4/17 (107)	106,377.2	469.0
	OS30	2018/7/11 (192)	66.73	168.96	42	Core	2018/5/17 (137)	59,460.1	1033.1
HLY 1801	DBO2-1	2018/8/9 (221)	64.67	169.93	48	Van Veen	2018/4/16 (106)	104,868.8	427.2
	DBO2-4	2018/8/9 (221)	64.96	169.90	49	Van Veen	2018/4/17 (107)	143,193.9	469.0
	DBO3-6	2018/8/10 (222)	67.90	168.25	59	Core	2018/5/20 (140)	95,858.0	935.9
	DBO3-7	2018/8/11 (223)	67.79	168.60	51	Core	2018/5/20 (140)	104,109.1	935.1
	IC-3	2018/8/13 (225)	71.60	165.30	43	Van Veen	2018/6/26 (177)	32,304.9	1829.9
	IC-8	2018/8/14 (226)	70.97	163.56	46	Van Veen	2018/6/30 (181)	48,394.7	1391.3
	DBO4-2	2018/8/15 (227)	71.22	161.29	50	Core	2018/7/14 (195)	17,824.0	1891.3
	DBO4-4	2018/8/15 (227)	71.48	161.50	49	Core	2018/7/15 (196)	15,406.3	2377.8
	DBO4-5	2018/8/15 (227)	71.61	161.62	47	Core	2018/7/14 (195)	19,747.3	2477.9
	DBO5-9	2018/8/17 (229)	71.58	157.82	66	Van Veen	2018/7/22 (203)	2915.4	2667.8
	DBO5-10	2018/8/17 (229)	71.63	157.90	64	Core	2018/7/22 (203)	2813.1	2669.9
	LB-11	2018/8/22 (234)	70.06	167.66	50	Van Veen	2018/5/13 (133)	95,614.2	973.8
	LB-9	2018/8/23 (235)	69.88	166.82	47	Van Veen	2018/5/12 (132)	105,276.1	877.1
	LB-7	2018/8/23 (235)	69.68	166.09	42	Van Veen	2018/5/11 (131)	96,511.2	800.6
HLY 1803	DBO6-1	2018/10/30 (303)	71.16	152.26	32	Van Veen	2018/7/29 (210)	42,213.8	2824.9
	DBO6-3	2018/10/30 (303)	71.25	152.17	48	Van Veen	2018/7/29 (210)	55,326.5	2829.3
	DBO6-5	2018/10/30 (303)	71.34	152.10	71	Van Veen	2018/8/5 (217)	63,070.1	2899.2
	DBO6-7	2018/10/31 (304)	71.42	152.04	194	Van Veen	2018/8/5 (217)	52,153.7	2902.0
	PRB-1	2018/11/2 (306)	70.69	148.44	26	Van Veen	2018/8/26 (238)	—	3,347.2
	PRB-2	2018/11/2 (306)	70.77	148.33	35	Van Veen	2018/9/3 (246)	17,622.4	3,465.0
	PRB-4	2018/11/2 (306)	70.90	148.14	45	Van Veen	2018/9/4 (247)	16,083.4	3,405.6
	PRB-7	2018/11/2 (306)	71.02	147.98	58	Van Veen	2018/9/6 (249)	19,897.2	3,490.4
	MCK-1	2018/11/4 (308)	69.82	139.61	38	Van Veen	2018/8/3 (215)	40,557.1	2240.4
	MCK-2	2018/11/4 (308)	69.90	139.49	44	Van Veen	2018/8/3 (215)	47,209.6	2111.3
	MCK-3	2018/11/4 (308)	69.94	139.39	55	Van Veen	2018/8/3 (215)	47,343.2	2113.9
	MCK-4	2018/11/4 (308)	69.97	139.30	60	Van Veen	2018/8/3 (215)	46,782.5	2113.9
	KTO-2	2018/11/5 (309)	70.28	143.93	38	Van Veen	2018/8/18 (230)	30,870.8	3,191.8
	KTO-3	2018/11/5 (309)	70.37	143.79	48	Van Veen	2018/8/21 (233)	14,101.3	3,247.5
	KTO-5	2018/11/5 (309)	70.56	143.61	110	Van Veen	2018/8/19 (231)	13,958.0	3,221.7
	PRW-1	2018/11/7 (311)	70.68	148.91	24	Van Veen	2018/8/28 (240)	115,525.9	3,369.1
	PRW-4	2018/11/7 (311)	70.82	148.84	33	Van Veen	2018/8/28 (240)	76,570.9	3,373.2
	PRW-7	2018/11/7 (311)	70.95	148.78	38	Van Veen	2018/9/3 (246)	26,140.8	3,474.0
	DBO5-1	2018/11/14 (318)	71.25	157.13	47	Van Veen	2018/7/22 (203)	79,117.8	2661.3
	DBO5-3	2018/11/14 (318)	71.33	157.31	91	Van Veen	2018/7/21 (202)	59,407.8	2637.3

Table 1
Continued

Cruise	Station	Date (Julian day)	Latitude (°N)	Longitude (°W)	Bottom depth (m)	Sample type	TSR (Julian day)	IP$_{eu}$ (mg C m^{-2})	GP (hours)
	DBO5-5	2018/11/14 (318)	71.41	157.49	128	Van Veen	2018/7/21 (202)	44,093.7	2639.4
	DBO5-7	2018/11/14 (318)	71.50	157.66	85	Van Veen	2018/7/22 (203)	35,765.2	2667.8
	DBO5-9	2018/11/14 (318)	71.58	157.83	66	Van Veen	2018/7/22 (203)	35,857.3	2667.8
	DBO3-1	2018/11/15 (319)	68.31	166.92	35	Van Veen	2018/5/5 (125)	196,800.9	812.4
	DBO3-5	2018/11/15 (319)	68.01	167.88	54	Van Veen	2018/5/6 (126)	212,878.6	828.9
	DBO3-8	2018/11/15 (319)	67.67	168.95	50	Van Veen	2018/5/21 (141)	179,194.6	1124.6

Note. In sample type column, "core" and "Van Veen" indicate that the samples were collected by multiple corer and Van Veen grab sampler, respectively. The timing of sea ice retreat (TSR) indicates the last day when the SIC fell below 20% prior to the observed annual sea-ice minimum across the study region during summer. IP$_{eu}$ indicates daily integrated values of primary production from TSR to the date of the in situ sediment sampling was conducted. The growth period of the ice-associated assemblages (GP) indicates the integrated daylength during the periods with SIC > 20% after the daylight hours exceed 10 h.

samples, a portion of the 0–3 cm layer was collected from the grab or the core and stored in air-tight amber jars at 1–4°C. The sediment samples were stored for more than one month in order to eliminate vegetative cells. Since the main driver of diatom resting stage formation is considered to be nitrogen depletion (Mc-Quoid & Hobson, 1996), most resting stages are thought to form in the water column rather than near the benthos, as nutrient concentrations are higher near the seafloor.

2.3. Quantification of Diatom Resting Stages

The abundance of viable resting stages of diatoms in the sediment samples was analyzed using the most probable number (MPN) method (Imai et al., 1984, 1990). Homogenized wet sediment samples were suspended in Whatman GF/F filtered sterile seawater at a concentration of 0.1 g mL^{-1} (=10^0 dilution), and the subsequent serial tenfold dilutions (10^{-1} to 10^{-6}) were made with modified SWM-3 medium (Table 2) (Chen et al., 1969; Itoh & Imai, 1987). Then 1 mL aliquots of diluted suspensions were inoculated into five replicate wells of disposable tissue culture plates (48 wells). Incubation was carried out at a temperature of 5°C and under white fluorescent light of 50 or 116 μmol photons m^{-2} s^{-1} with a 14 h light:10 h dark photocycle for 10 days. The appearance of vegetative cells of planktonic diatoms in each well was examined using an inverted optical microscope. The most probable number (MPN for a series of 5 tenfold dilutions) of diatoms of each species in the sediment sample (MPN cells g^{-1} wet sediment) was then calculated according to the statistical table by Throndsen (1978). Since we observed wells with 10^{-2}–10^{-6} dilutions, the detectable cell numbers by the MPN method were from 1.8×10^2 to 2.4×10^7 MPN cells g^{-1} for each species. Note that we used the data set of Fukai et al. (2019) for the *Oshoro-Maru* expedition.

2.4. Statistical Analyses

The diatom resting stage communities were distinguished by cluster analysis. To reduce the bias for abundant species, the cell concentration data (X: MPN cells g^{-1} wet sediment) for each species were transformed to $\sqrt[4]{X}$ prior to cluster analysis (Quinn & Keough, 2002). Dissimilarities between samples were examined using the Bray-Curtis index based on the differences in the species composition. To group the samples, the dissimilarity indices were coupled using hierarchical agglomerative clustering with a complete linkage method (an unweighted pair group method using the arithmetic mean). A Mann-Whitney U-test was conducted to evaluate environmental factors (the TSR, IP$_{eu}$, and the growth period of ice-associated assemblages (GP)) between the distinguished groups. The GP was defined as the integrated daylength during the periods with SIC >20% after the daylight exceeded 10 h, as Gilstad and Sakshaug (1990) indicated that ice-associated assemblages could increase their growth rate when daylight hours exceeded 10 h.

We defined the open-water assemblages as the community with centric diatoms, excluding *Attheya* spp., and the ice-associated assemblages as the community with pennate diatoms and *Attheya* spp., as *Attheya*
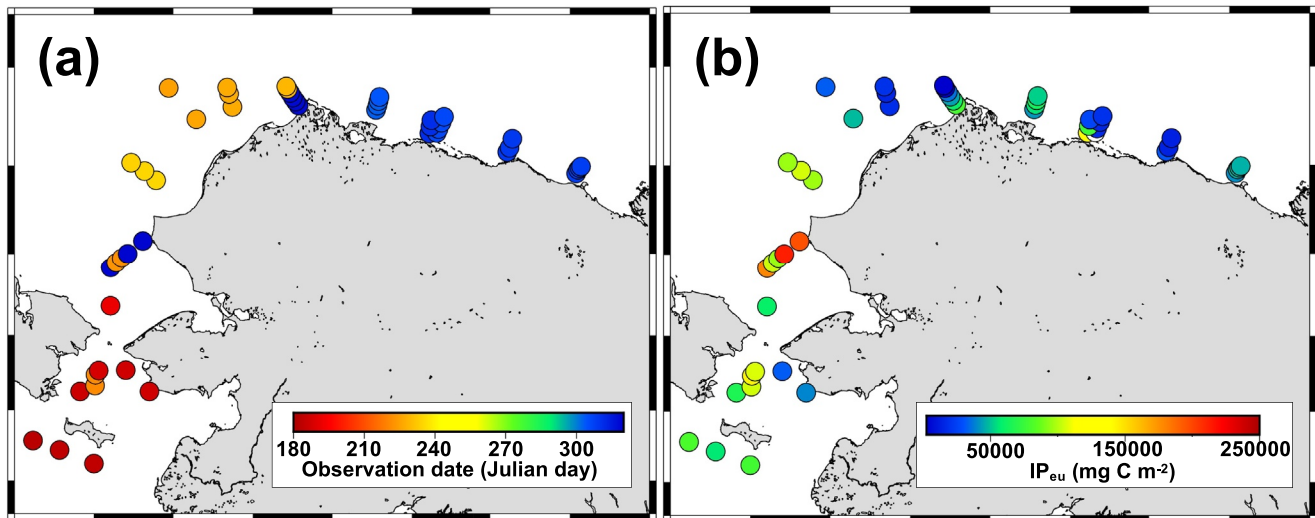
Figure 2. (a) Horizontal values of the observation date (b) and the daily cumulative euphotic-depth-integrated primary production from the TSR to the observation date (IP$_{eu}$).

spp. and pennate diatoms are often reported to be present in the sea-ice (e.g., Campbell et al., 2018; Melnikov et al., 2002; von Quillfeldt et al., 2003; Szymanski & Gradinger, 2016; Werner et al., 2007). Based on this definition, we analyzed the relationships of ice-associated assemblages with the TSR and the GP using Spearman's rank correlation coefficient.

All statistical analyses were conducted using R software (version 3.6.1, R Development Core Team, 2019).

Table 2
Components of the Modified SWM-3 Medium (Left Column) and Detail Components of P1-Metals and S-3 Vitamin (Right Column).

Component	Concentrations in final medium / Amounts per litter	Component	Concentrations/ Amounts
NaNO$_3$	2.0 mM	P-1 metal in10 mL	
NaH$_2$PO$_4$·2H$_2$O	0.1 mM	H$_3$BO$_3$	1.0 mM
Na$_2$SiO$_3$·9H$_2$O	0.2 mM	MnCl$_2$·4H$_2$O	3.5×10^{-2} mM
Na$_2$EDTA	30.0 μM	ZnCl$_2$	4.0×10^{-3} mM
Fe-EDTA	2.0 μM	CoCl$_2$·6H$_2$O	1.0×10^{-4} mM
Na$_2$SeO$_3$	2.0 nM	CuCl$_2$·2H$_2$O	1.0×10^{-6} mM
Na$_2$MoO$_4$·2H$_2$O	100 nM	S-3 Vitamin in 2 mL	
TRIS	500 mg	B$_1$-HCl	0.5 mg
P1-metals	10.0 mL	Ca-Pantothenate	0.1 mg
S-3 Vitamins	2.0 mL	Nicotinic acid	0.1 mg
		P-Aminobenzoic acid	10.0 μg
		Biotin	1.0 μg
		Inositol	5.0 mg
		Folic acid	2.0 μg
		Thymine	3.0 mg
		Vitamin B$_{12}$	1.0 μg

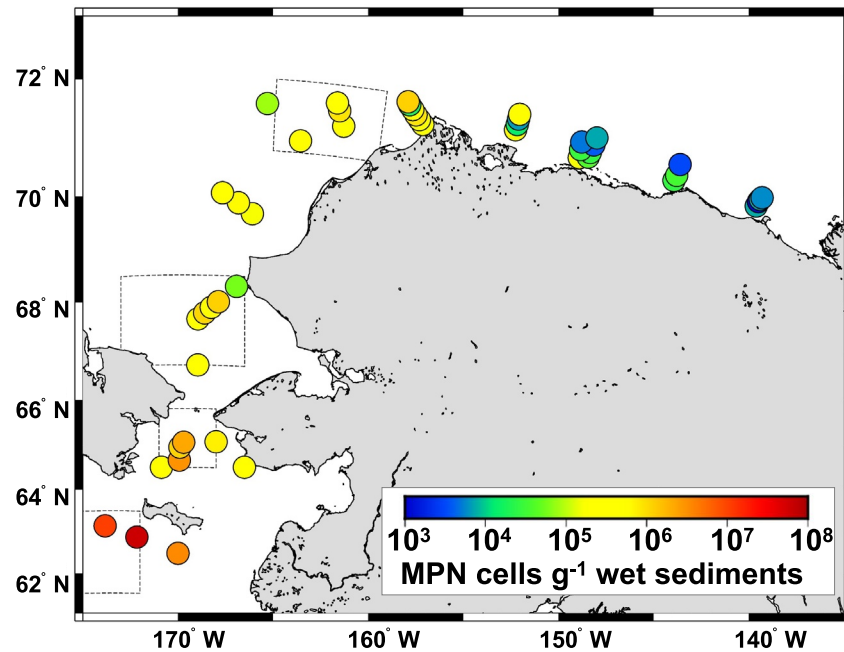*Note.* Solvent of the medium is natural filtered sea water. Medium pH is 7.8.

Figure 3. Horizontal distribution of diatom resting stages in the north Bering, Chukchi and Beaufort Seas in 2018. Squares indicate benthic hot spots indicated by Grebmeier et al. (2015).

3. Results

3.1. Sea-Ice and Primary Production

The TSR was different among regions (Table 1). The sea-ice retreated from south to north in the northern Bering and the Chukchi Seas, and from west to east in the southwestern Beaufort Sea (Figure 1).

The IP_{eu} had a regional feature in which high values were observed in the southern Chukchi Sea and low values in the southwestern Beaufort Sea (Table 1, Figure 2b).

3.2. Diatom Concentrations and Species Composition

The viable diatom resting stages determined by the MPN method ranged over four orders of magnitude, from 1.21×10^3 to 6.1×10^7 MPN cells g^{-1} wet sediment (Figure 3). Highest concentrations were found to the south of St. Lawrence Island (3.4×10^6–6.1×10^7 MPN cells g^{-1} wet sediment). In the Chirikov Basin, which extends northwards from St. Lawrence Island to the Bering Strait (DBO2-1, DBO2-4, OS14, OS19, OS20, OS22), diatom concentrations were relatively high (2.8×10^5–3.0×10^6 MPN cells g^{-1} wet sediments). Diatom concentrations near Utqiagvik (DBO5-10) were also relatively high (1.2×10^6 MPN cells g^{-1} wet sediments). In contrast, cell concentrations were lower in samples from the coastal region of the southwestern Beaufort Sea (DBO6-5, PRW-7, PRB-4, PRB-7, KTO-5, MCK-1, MCK-2, MCK-3, MCK-4) (1.2×10^3–7.8×10^3 MPN cells g^{-1} wet sediments). 19 genera and 20 species were observed over the study region - 12 genera and 14 species of centric diatoms and 7 genera and 6 species of pennate diatoms. Centric diatoms were dominant at almost all stations, although dominant species varied geographically; proportional abundance of *Chaetoceros* spp. and *Thalassiosira* spp. were found in samples collected from the northern Bering Sea and Chukchi Sea, whereas *Attheya* spp. were highest in the southwestern Beaufort Sea (Figure 4). Pennate diatoms comprised over 50% of the diatom assemblages at some stations (DBO4-4, MCK-1, MCK-2, MCK-3), with highest proportional abundance found in samples from the southwestern Beaufort coastal region (Figure 4). Total cell concentration in sediments were positively correlated with the cell concentrations of *Chaetoceros* spp. and *Thalassiosira* spp. (Spearman, $\rho = 0.97$, $p < 0.05$) (Figure 5).

In order to test for seasonal effects, diatom assemblages were compared over time in stations in the northern Bering Sea and Southern Chukchi Sea, which included locations from each sampling period (OS14, 19, 20,
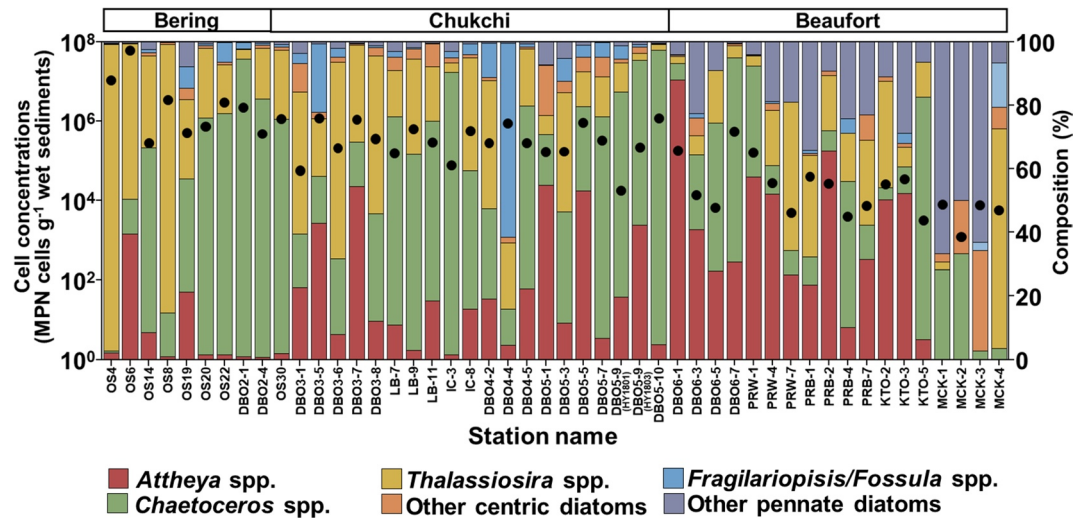
Figure 4. Cell concentrations and species composition of diatom resting stages in the northern Bering, Chukchi and Beaufort Seas in 2018.

22, 30 by *Oshoro-Maru*, DBO2-1, 2–4, 3–6, 3–8 in HLY 1801, and DBO 3–1, 3–5, 3–7 in HLY 1803). There were no significant differences in species or genera among these samples (one-way ANOVA, $p > 0.05$), with the exception of *Attheya* spp. and *C. debilis* (one-way ANOVA, $p < 0.05$).

3.3. Diatom Assemblages by Cluster Analysis

Cluster analysis based on concentrations of diatom resting stages classified the diatom assemblages into two groups (A, B) and four outgroups at 52% dissimilarity levels. Group A was distributed from the northern Bering Sea to the Chukchi Sea near Utqiagvik (Figure 6a). Cell concentrations in group A were very high (7.9×10^4–1.1×10^7 MPN cells g^{-1} wet sediments, avg = 1.2×10^6 MPN cells g^{-1} wet sediment), and samples in this group with dominated by *Chaetoceros* spp. and *Thalassiosira* spp. (35% and 51%, respectively) (Figure 6b). Group B included stations from the southwestern Beaufort Sea, where cell concentrations ranged from 3.2×10^3 to 2.1×10^5 MPN cells g^{-1} wet sediment (avg = 5.8×10^4 MPN cells g^{-1} wet sediment) and *Attheya* spp. were dominant (47%) (Figure 6b). All stations from the easternmost transect in the study region (MCK) were classified as outgroups (Figure 6a).

3.4. Relationships With Environmental Factors

Environmental factors differed between samples comprising diatom groups A and B. The TSR was significantly later at the group B locations compared to group A (*U*-test, $p < 0.05$) (Figure 7a), and the GP was significantly longer at group B locations than group A (*U*-test, $p < 0.05$) (Figure 7b). The switching between the two diatom groups occurred around 200 Julian day of the TSR and approximately 2500 h of the GP (Figures 7a, 7b and 8). By contrast, the IP$_{eu}$ and the sampling depth were not significantly different between groups (*U*-test, $p > 0.05$) (Figures 7c and 7d).

In addition, the TSR and the GP were significantly positively correlated with the proportion of pennate diatoms and *Attheya* spp., which are defined as the ice-associated assemblages ($\rho = 0.63$ and 0.29, respectively, $p < 0.05$) (Figure 8).
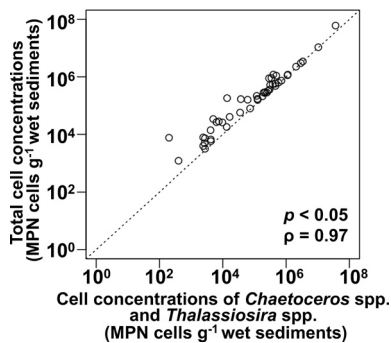

Figure 5. The relationship between the abundances of *Chaetoceros* spp. and *Thalassiosira* spp. and total cell concentrations in most probable number.
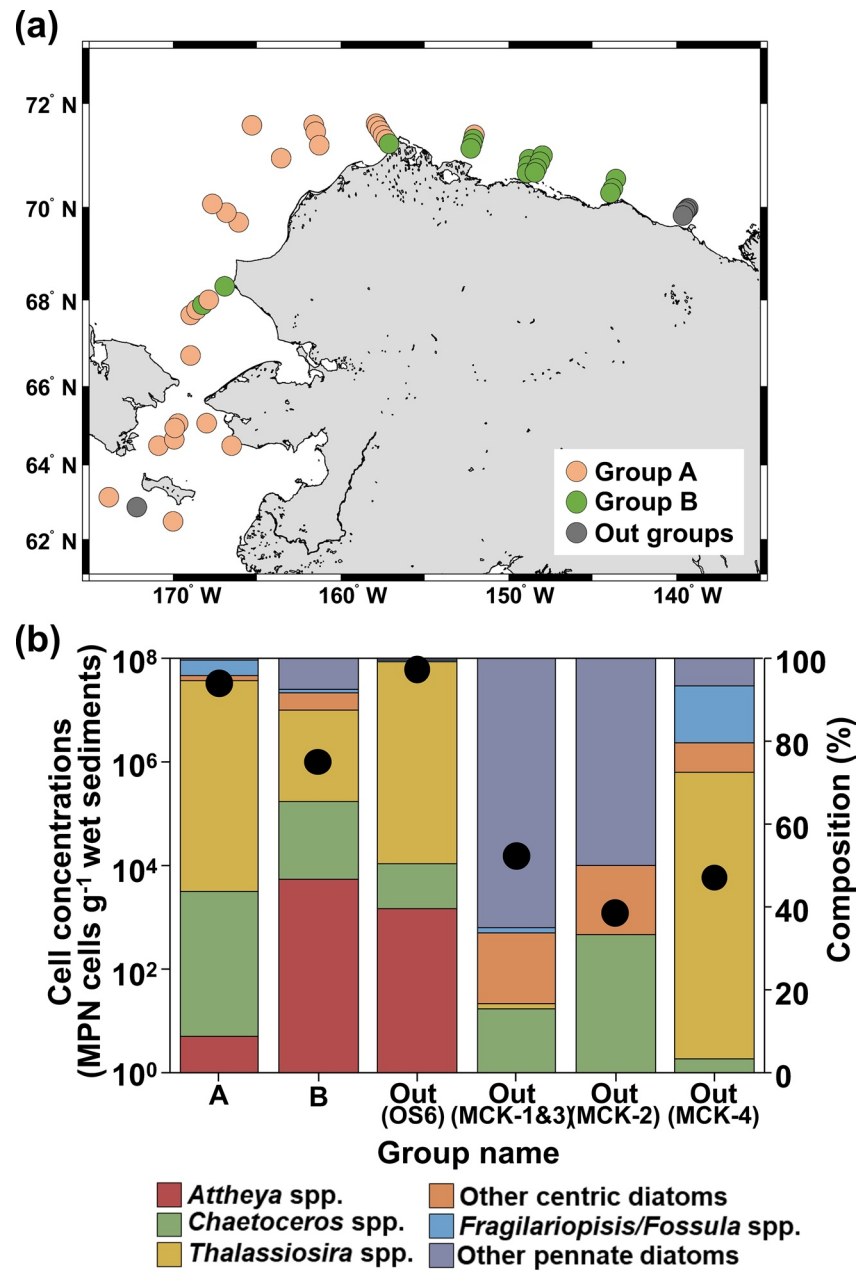
Figure 6. (a) Spatial distribution of diatom resting stage communities by group. (b) Species composition and cell concentrations in each group.

4. Discussion

Examination of the distribution and abundance of diatom resting stages in Pacific Arctic sediments demonstrated a strong correlation with the timing of sea ice retreat and the growth period of ice-associated assemblages. Details regarding spatial community dynamics and relationships between diatom assemblages and TSR, GP, and environmental parameters are discussed below.
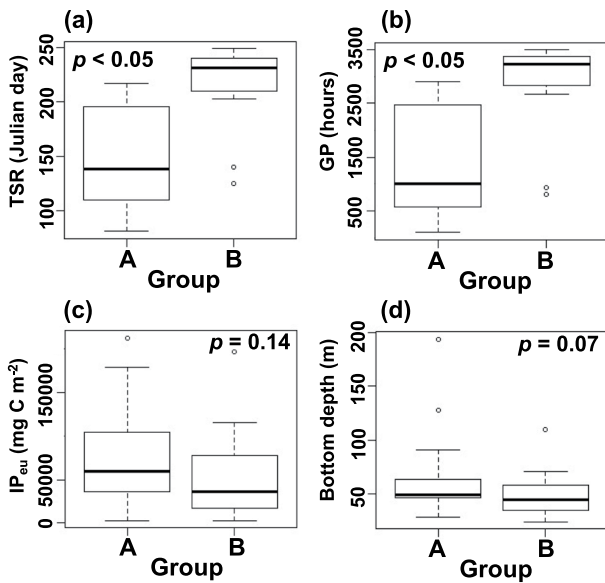
Figure 7. Comparison of environmental factors between diatom resting stage groups. (a) The timing of the sea-ice retreat (TSR). (b) The growth period of ice-associated assemblages (GP). (c) The daily cumulative euphotic-depth-integrated primary production from the TSR to the observation date (IP_{eu}). (d) The bottom depth of sampling station.

4.1. Distribution of Diatom Resting Stages and the Relationships With Primary Production in the Pacific Arctic Region

Cell concentrations of diatom resting stages exhibited geographic variability that roughly corresponded with levels of primary production previously reported in the region. However, primary production values estimated by satellite remote sensing in this study did not have any statistically significant relationships with diatom resting stage assemblages.

This study found high concentrations of diatom resting stages in the northern Bering Sea and the Chukchi Sea (avg = 3.1×10^6 MPN cells g^{-1} wet sediments), but low concentrations (avg = 6.2×10^4 MPN cells g^{-1} wet sediments) in the southwestern Beaufort Sea. This is consistent with prior studies of primary productivity that documented high annual water-column integrated primary production in the northern Bering and Chukchi Seas and low productivity in the western Beaufort Sea (Grebmeier et al., 2006; Hill et al., 2018). However, we did not find a significant relationship between diatom resting stage assemblages and primary production values estimated by satellite. O'Daly et al. (2020) presented similar findings; that higher rates of primary productivity were correlated with higher rates of POC flux, including viable diatoms, but that there is variability in the export efficiency. Thus, while the hypothesis that diatom resting stage concentrations reflect primary productivity in the water column (Imai et al., 1990; Itakura et al., 1997; Pitcher, 1990) holds up over broad features of the Pacific Arctic region, additional data are needed to justify this using resting stage assemblages as a strict proxy for productivity.

Another cause of high concentrations of resting stages observed in the northern Bering and Chukchi Seas is related to the high sinking flux in this region (O'Daly et al., 2020). Lalande et al. (2020) used a time series of sediment trap observations at single station in the Chukchi Sea to show that diatoms make up a high proportion of POC flux. The characteristically high sinking flux in the northern Bering and Chukchi Seas could drive high concentrations of sediment diatom assemblages reported here, though diatom losses by zooplankton grazing also need to be considered (Campbell et al., 2009; Sherr et al., 2009).

We considered the impact that variable sampling times may have had upon the assemblages observed in this study. The sediments were obtained over several different time periods (July 2–12, 2018, August 9–23, 2018, and October 30 to November 15, 2018), and it is possible that the community structure changed from summer to fall. However, there were no significant differences in species or genera except for *Attheya* spp. and *C. debilis* between samples at replicated stations in the northern Bering Sea and Southern Chukchi Sea,
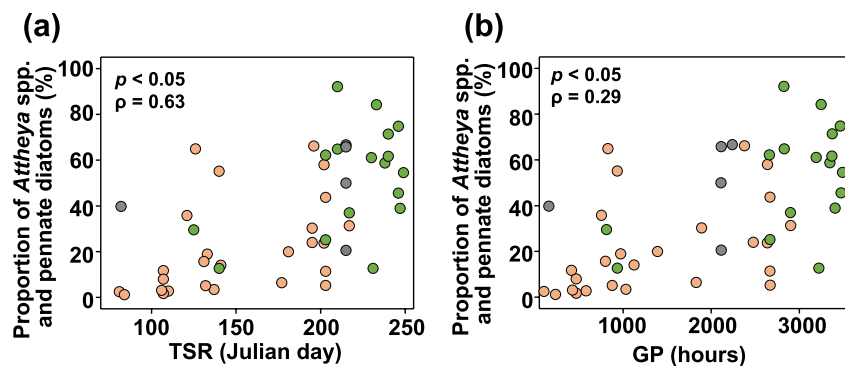

Figure 8. Relationships between the proportion of the ice-associated species (*Attheya* spp. and pennate diatoms) in most probable number and the timing of the sea-ice retreat (a), and the GP (b). Each color indicate the diatom groups (pink: group A, green: group B, and gray: out groups).

where sampling was conducted over multiple time periods. Dissimilarity among almost all the samples was less than 40%, and they were also grouped in the cluster analysis. Water temperature is known to influence resting stage survival time, with colder water increasing survival time length (McQuoid & Hobson, 1996). Hargraves and French (1983) reported that *Chaetoceros diadema*, *Detonula confervacea*, *Leptocylindrus danicus,* and *Thalassiosira nordenskioeldii*, which sometimes appear in the Pacific Arctic sediments, survived for 291, 220, 400, and 220 days, respectively, at temperatures between 5–6°C. These periods are sufficiently longer than the difference in sampling periods (the longest difference is 136 days). Given that temperatures at the seafloor of the Pacific Arctic are lower than 5–6°C, we do not believe that the survival time of resting stages impacted our results. For these reasons, differences over sampling periods appeared to be almost negligible in this study.

4.2. The Relationship of Diatom Resting Stage Assemblages With the TSR and the GP

Prior investigators have shown that the magnitude and composition of diatom assemblages in the Arctic spring bloom are influenced by the presence of the sea-ice and the timing of the sea-ice retreat (Fujiwara et al., 2016; Fukai et al., 2019; Neeley et al., 2018). In this study, the distribution of diatom resting stage assemblages were clearly related to spatial differences in the TSR. In locations where the ice retreat was early, such as the northern Bering and the Chukchi Seas, *Chaetoceros* spp. including *C. socialis s.l.* and *Thalassiosira* spp. were dominant in sediments (*C. socialis s.l.*: 0.36–93.1%, *Chaetoceros* spp.: 0.76–93.6%, *Thalassiosira* spp.: 2.0–96.4%). Because they are known to form dense spring blooms in these regions (von Quillfeldt, 2000; Sergeeva et al., 2010), these data suggest that diatom resting stages were formed and settled to the seafloor after spring blooms of *Chaetoceros* spp. and *Thalassiosira* spp. in the northern Bering Sea and the Chukchi Sea. In addition, the positive correlation between *Chaetoceros* spp. and *Thalassiosira* spp. cell concentrations with total cell concentrations indicates that where the TSR was early and the open-water period was long, large diatom blooms of *Chaetoceros* spp. and *Thalassiosira* spp. produced high quantities of resting stage cells (Fukai et al., 2019).

The TSR had also an effect on the diatom community composition, especially the proportion of ice-associated diatoms in diatom assemblages. In the southwestern Beaufort Sea, where the TSR was late, diatom assemblages were dominated by ice-associated species (Groups B and outgroups in the transect MCK), again demonstrating that sea-ice is a driver of benthic community structure among the exported diatoms. In addition, the prevalence of ice-associated species was positively correlated with the TSR, suggesting that the proportion of ice algae in diatom assemblages is higher when sea-ice persists. This is likely due in part to their ability to sustain growth under low light levels (<1 μmol photon s^{-1} m^{-2}) (Cota & Smith, 1991; Mock & Gradinger, 1999); notably, Tsukazaki et al. (2018) demonstrated that the centric genus *Attheya* spp. could survive in dark for more than six months, and thus can withstand low light conditions in the Arctic. It is possible that this study underestimated the concentrations of pennate diatoms in sediments compared with *Attheya* spp. and other centric diatoms, as few marine pennate diatoms are known to form resting stages, while many centric diatoms do (McQuoid & Hobson, 1996), and the fate of the pennate diatoms in sediment is largely unknown. Despite this potential bias, these data indicate that the proportion of ice-associated species was higher where the TSR occurred later. Interestingly, a spatial change from the assemblage dominated by open-water species to that with high proportion of ice-associated diatoms occurred at stations where the TSR was around the 200th Julian day (mid-July). This indicates a potential threshold between dominant diatom groups based on the TSR parameter.

For ice-associated assemblages in the surface sediments, the length of the growth period during which algae receive sufficient light before the TSR is important (Fukai et al., 2019). The proportional abundance of ice-associated diatoms was significantly higher when GP was longer, suggesting that photoperiod during sea-ice presence is another important driver of diatom community structure (Cota & Home, 1989; Gosselin et al., 1990; Smith et al., 1988). In addition, a GP boundary of 2500 h may be an important parameter for the distribution of ice-associated assemblages due to corresponding changes that were observed. Future efforts to evaluate and predict diatom assemblages should consider both the TSR and the GP.

4.3. Connecting Diatom Distribution to Higher Trophic Levels

The diatom assemblages had clear relationships with the TSR and the GP. In the northern Bering Sea, the early timing of the sea-ice retreat and subsequent changes in diatom assemblages in the water column and the sediment was reported in 2018 (Fukai et al., 2019, 2020). This indicates that the recent drastic reduction of sea-ice in the Pacific Arctic region may induce a shift in diatom assemblages from relative dominance of ice-associated species to open-water species.

The distribution and composition of diatom species in this study were associated with the zooplankton feeding environment in the Pacific Arctic region. As diatoms comprise the largest portion of the mesozooplankton diet, especially in spring (Campbell et al., 2016), changes in diatom species composition will perturb prey environments of higher trophic-level organisms. The spatial trend of diatom resting stage concentrations exhibited a similar gradient to zooplankton $\delta^{13}C$ values showed by Pomerleau et al. (2014), which reported values that were more enriched in the western Bering Strait and less enriched on the Beaufort shelf. Nakatsuka et al. (1992) reported an increase in $\delta^{13}C$ of POC during a diatom bloom in a mesocosm experiment in Saanich Inlet, Canada. Additionally, they showed that the main factor influencing the variation of $\delta^{13}C$ of POC during a phytoplankton bloom in a mesocosm experiment was the specific production rate of POC, which can be proportional to the specific growth rate of phytoplankton, rather than carbon dioxide system or community composition (Nakatsuka et al., 1992). Typically, fast-growing diatoms (e.g., *Chaetoceros* spp. and *Thalassiosira* spp.) and zooplankton that feed on these diatoms are enriched with ^{13}C (Fry & Wainright, 1991). The inflow of nutrient rich Anadyr waters from the western Bering Strait is known to fuel huge blooms of *Chaetoceros* spp. and *Thalassiosira* spp. (Danielson et al., 2017; Sergeeva et al., 2010), explaining the high concentrations of these species in sediments of the northern Bering and the Chukchi Seas reported here. In addition, regions of high diatom resting stage concentrations roughly corresponded to benthic hotspots, which include waters to the south of St. Lawrence Island, the Chirikov Basin, the southeastern Chukchi Sea and the northeastern Chukchi Sea (Grebmeier et al., 2015). In these regions with mean depths from 43 to 65 m, benthic primary production can be lower than pelagic production due to light limitation, and accumulation of microalgae in sediments are the main food source for benthic communities (Grebmeier et al., 2015). In particular, diatoms are valuable taxa because they are rich in polyunsaturated fatty acids (PUFAs) (Brown et al., 1997). Furthermore, Wang et al. (2016) analyzed the blubber fatty acid composition and stable carbon isotope ratios of ice seals, who feed on pelagic and benthic fishes, in the northern Bering and the southern Chukchi Seas to show that ice algae production contributed up to 80% of ice seal diets through trophic transfer. Therefore, changes in diatom assemblages caused by sea-ice dynamics will directly influence zooplankton and benthos production, with indirect effects upon higher trophic levels.

5. Conclusions

This study demonstrated that the distribution and community composition of diatom resting stages in the Pacific Arctic region were significantly influenced by the presence of sea-ice and the light environment. Diatom resting stages appear to follow broad spatial patterns of primary productivity across the region, suggesting the potential use of diatom resting stages as one of the proxies for productivity, despite the fact that there was not a significant relationship between diatom assemblages and primary productivity estimated by satellite observations. The TSR and the GP were important drivers of diatom assemblages, and significantly influenced the composition of diatoms in sediments. In particular, diatom assemblages changed spatially from composition dominated by open-water species to a high proportion of ice-associated diatoms in the region where the TSR occurred after mid-July (around the 200th Julian day) and the GP was over 2500 h. This result may indicate that a shift to earlier TSR under future climate conditions could induce not only delayed bloom timing (Hirawake & Hunt, 2020; Kikuchi et al., 2020) but also a change in the composition of diatom assemblages forming the spring bloom. The distribution of diatom resting stages is a valuable approach for investigating the diatom community, particularly on the Arctic shelves where it is logistically challenging to characterize the rapid seasonal succession in community composition that occurs across this remote and dynamic geographic region. Moreover, this approach provides species-level resolution lacking in satellite observations, providing a more robust assessment of the ecosystem implications of community changes. On the ecosystem level, it is interesting that the distribution of diatom resting stages corresponded

spatially with benthic hot spots and the feeding environment of zooplankton. Based on this research, it is clear that future changes in sea-ice extent and duration will impact diatom communities, and that resulting fluctuations in primary productivity and community structure will affect other components of Arctic marine ecosystems.

Data Availability Statement

The data reported in this paper have been deposited in the data archive site of Hokkaido University, http://hdl.handle.net/2115/80394.

References

Arrigo, K. R., van Dijken, G., & Pabi, S. (2008). Impact of a shrinking Arctic ice cover on marine primary production. *Geophysical Research Letters*, *35*(19), L19603. https://doi.org/10.1029/2008GL035028

Brock, T. D. (1981). Calculating solar radiation for ecological studies. *Ecological Modelling*, *14*(1), 1–19. https://doi.org/10.1016/0304-3800(81)90011-9

Brown, M. R., Jeffrey, S. W., Volkman, J. K., & Dunstan, G. A. (1997). Nutritional properties of microalgae for mariculture. *Aquaculture*, *151*(1–4), 315–331. https://doi.org/10.1016/S0044-8486(96)01501-3

Campbell, K., Mundy, C. J., Belzile, C., Delaforge, A., & Rysgaard, S. (2018). Seasonal dynamics of algal and bacterial communities in Arctic sea ice under variable snow cover. *Polar Biology*, *41*(1), 41–58. https://doi.org/10.1007/s00300-017-2168-2

Campbell, R. G., Ashjian, C. J., Sherr, E. B., Sherr, B. F., Lomas, M. W., Ross, C., et al. (2016). Mesozooplankton grazing during spring sea-ice conditions in the eastern Bering Sea. *Deep Sea Research Part II: Topical Studies in Oceanography*, *134*, 157–172. https://doi.org/10.1016/j.dsr2.2015.11.003

Campbell, R. G., Sherr, E. B., Ashjian, C. J., Plourde, S., Sherr, B. F., Hill, V., & Stockwell, D. A. (2009). Mesozooplankton prey preference and grazing impact in the western Arctic Ocean. *Deep Sea Research Part II: Topical Studies in Oceanography*, *56*(17), 1274–1289. https://doi.org/10.1016/j.dsr2.2008.10.027

Chen, L. C.-M., Edelstein, T., & McLachlan, J. (1969). Bonnemaisonia Hamifera Hariot in Nature and in culture. *Journal of Phycology*, *5*(3), 211–220. https://doi.org/10.1111/j.1529-8817.1969.tb02605.x

Cota, G. F., & Home, E. (1989). Physical control of Arctic ice algal production. *Marine Ecology Progress Series*, *52*, 111–121. https://doi.org/10.3354/meps052111

Cota, G. F., & Smith, R. E. H. (1991). Ecology of bottom ice algae: II. Dynamics, distributions and productivity. *Journal of Marine Systems*, *2*(3), 279–295. https://doi.org/10.1016/0924-7963(91)90037-U

Danielson, S. L., Eisner, L., Ladd, C., Mordy, C., Sousa, L., & Weingartner, T. J. (2017). A comparison between late summer 2012 and 2013 water masses, macronutrients, and phytoplankton standing crops in the northern Bering and Chukchi Seas. *Deep Sea Research Part II: Topical Studies in Oceanography*, *135*, 7–26. https://doi.org/10.1016/j.dsr2.2016.05.024

Durbin, E. G. (1978). Aspects of the biology of resting spores of Thalassiosira nordenskioeldii and Detonula confervacea. *Marine Biology*, *45*(1), 31–37. https://doi.org/10.1007/BF00388975

Frey, K. E., Comiso, J. C., Cooper, L. W., Grebmeier, J. M., & Stock, L. V. (2018). *Arctic ocean primary productivity: The response of marine algae to climate warming and sea ice decline, 7*.

Frost, K. J., & Lowry, L. F. (1984). Trophic relationships of vertebrate consumers in the Alaskan Beaufort Sea. In P. W. Barnes, D. M. Schell, & E. Reimnitz (Eds.), *The alaskan Beaufort Sea: Ecosystems and environments* (pp. 381–401). Academic Press. https://doi.org/10.1016/b978-0-12-079030-2.50024-1

Fry, B., & Wainright, S. C. (1991). Diatom sources of 13 C-rich carbon in marine food webs. *Marine Ecology Progress Series*, *76*(2), 149–157. https://doi.org/10.3354/meps076149

Fujiwara, A., Hirawake, T., Suzuki, K., Eisner, L., Imai, I., Nishino, S., et al. (2016). Influence of timing of sea ice retreat on phytoplankton size during marginal ice zone bloom period on the Chukchi and Bering shelves. *Biogeosciences*, *13*(1), 115–131. https://doi.org/10.5194/bg-13-115-2016

Fukai, Y., Abe, Y., Matsuno, K., & Yamaguchi, A. (2020). Spatial changes in the summer diatom community of the northern Bering Sea in 2017 and 2018. *Deep Sea Research Part II: Topical Studies in Oceanography*, *181–182*, 104903. https://doi.org/10.1016/j.dsr2.2020.104903

Fukai, Y., Matsuno, K., Fujiwara, A., & Yamaguchi, A. (2019). The community composition of diatom resting stages in sediments of the northern Bering Sea in 2017 and 2018: The relationship to the interannual changes in the extent of the sea ice. *Polar Biology*, *42*(10), 1915–1922. https://doi.org/10.1007/s00300-019-02552-x

Garrison, D. L. (1984). *Chapter 1, Planktonic diatoms*. Marine Plankton Life Cycle Strategies (Vol. 1–17).

Gilstad, M., & Sakshaug, E. (1990). Growth rates of ten diatom species from the Barents Sea at different irradiances and day lengths. *Marine Ecology Progress Series*, *64*, 169–173. https://doi.org/10.3354/meps064169

Gosselin, M., Legendre, L., Therriault, J.-C., & Demers, S. (1990). Light and nutrient limitation of sea-ice microalgae (Hudson Bay, Canadian Arctic)1. *Journal of Phycology*, *26*(2), 220–232. https://doi.org/10.1111/j.0022-3646.1990.00220.x

Grebmeier, J. M., Bluhm, B. A., Cooper, L. W., Danielson, S. L., Arrigo, K. R., Blanchard, A. L., et al. (2015). Ecosystem characteristics and processes facilitating persistent macrobenthic biomass hotspots and associated benthivory in the Pacific Arctic. *Progress in Oceanography*, *136*, 92–114. https://doi.org/10.1016/j.pocean.2015.05.006

Grebmeier, J. M., Cooper, L. W., Feder, H. M., & Sirenko, B. I. (2006). Ecosystem dynamics of the Pacific-influenced Northern Bering and Chukchi Seas in the Amerasian Arctic. *Progress in Oceanography*, *71*(2–4), 331–361. https://doi.org/10.1016/j.pocean.2006.10.001

Grebmeier, J. M., McRoy, C., & Feder, H. (1988). Pelagic-benthic coupling on the shelf of the northern Bering and Chukchi Seas. I. Food supply source and benthic bio-mass. *Marine Ecology Progress Series*, *48*, 57–67. https://doi.org/10.3354/meps048057

Hargraves, P. E., & French, F. W. (1983). Diatom resting spore: Significance and strategies. In G. A. Fryxell (Ed.), *Survival strategies of the algae* (pp. 49–68). Cambridge University Press.

Hill, V., Ardyna, M., Lee, S. H., & Varela, D. E. (2018). Decadal trends in phytoplankton production in the Pacific Arctic Region from 1950 to 2012. *Deep Sea Research Part II: Topical Studies in Oceanography*, *152*, 82–94. https://doi.org/10.1016/j.dsr2.2016.12.015

Hirawake, T., & Hunt, G. L. (2020). Impacts of unusually light sea-ice cover in winter 2017-2018 on the northern Bering Sea marine ecosystem—An introduction. *Deep Sea Research Part II: Topical Studies in Oceanography*, *181–182*, 104908. https://doi.org/10.1016/j.dsr2.2020.104908

Hirawake, T., Shinmyo, K., Fujiwara, A., & Saitoh, S. (2012). Satellite remote sensing of primary productivity in the Bering and Chukchi Seas using an absorption-based approach. *ICES Journal of Marine Science*, *69*(7), 1194–1204. https://doi.org/10.1093/icesjms/fss111

Hollibaugh, J. T., Seibert, D. L. R., & Thomas, W. H. (1981). Observations on the survival and germination of resting spores of three Chaetoceros (Bacillariophyceae) species1, 2. *Journal of Phycology*, *17*(1), 1–9. https://doi.org/10.1111/j.1529-8817.1981.tb00812.x

Horner, R. (1984). Phytoplankton abundance, chlorophyll a, and primary production in the western Beaufort Sea. In P. W. Barnes, D. M. Schell, & E. Reimnitz (Eds.), *The alaskan Beaufort Sea: Ecosystems and environments* (pp. 295–310). Academic Press. https://doi.org/10.1016/b978-0-12-079030-2.50020-4

Horner, R., & Schrader, G. C. (1982). Relative Contributions of Ice Algae, Phytoplankton, and Benthic Microalgae to Primary Production in Nearshore Regions of the Beaufort Sea. *ARCTIC*, *35*(4), 485–503. https://doi.org/10.14430/arctic2356

Imai, I., Itakura, S., & Itoh, K. (1990). Distribution of diatom resting cells in sediments of Harima-Nada and northern Hiroshima Bay, the Seto Island Sea, Japan. *Bulletin on coastal oceanography*, *28*(1), 75–84. https://doi.org/10.32142/engankaiyo.28.1_75

Imai, I., Itoh, K., & Anraku, M. (1984). Extinction dilution method for enumeration of dormant cells of Red Tide organisms in marine sediments. *Bulletin of Plankton Society of Japan*, *312*, 123–124.

Itakura, S., Imai, I., & Itoh, K. (1997). "Seed bank" of coastal planktonic diatoms in bottom sediments of Hiroshima Bay, Seto Inland Sea, Japan. *Marine Biology*, *128*(3), 497–508. https://doi.org/10.1007/s002270050116

Itoh, K., & Imai, I. (1987). Rafido-So. In The Japan fisheries resources conservation association. (Ed.), *A guide for studies of red tide organisms* (pp. 122–130). Shuwa.

Kikuchi, G., Abe, H., Hirawake, T., & Sampei, M. (2020). Distinctive spring phytoplankton bloom in the Bering Strait in 2018: A year of historically minimum sea ice extent. *Deep Sea Research Part II: Topical Studies in Oceanography*, *181–182*, 104905. https://doi.org/10.1016/j.dsr2.2020.104905

Lalande, C., Grebmeier, J. M., Hopcroft, R. R., & Danielson, S. L. (2020). Annual cycle of export fluxes of biogenic matter near Hanna Shoal in the northeast Chukchi Sea. *Deep Sea Research Part II: Topical Studies in Oceanography*, *177*, 104730. https://doi.org/10.1016/j.dsr2.2020.104730

Lee, Z., Lubac, B., Werdell, J., & Arnone, R. (2009). *An update of the quasi-analytical Algorithm (QAA_v5)*. Retrieved January 6, 2021, from http://www.ioccg.org/groups/software.html

Lee, Z., Weidemann, A., Kindle, J., Arnone, R., Carder, K. L., & Davis, C. (2007). Euphotic zone depth: Its derivation and implication to ocean-color remote sensing. *Journal of Geophysical Research: Oceans*, *112*(C3). https://doi.org/10.1029/2006JC003802

Markus, T., Stroeve, J. C., & Miller, J. (2009). Recent changes in Arctic sea ice melt onset, freezeup, and melt season length. *Journal of Geophysical Research: Oceans*, *114*(C12). https://doi.org/10.1029/2009JC005436

McQuoid, M. R., & Hobson, L. A. (1996). Diatom resting stages. *Journal of Phycology*, *32*(6), 889–902. https://doi.org/10.1111/j.0022-3646.1996.00889.x

Melnikov, I. A., Kolosova, E. G., Welch, H. E., & Zhitina, L. S. (2002). Sea ice biological communities and nutrient dynamics in the Canada Basin of the Arctic Ocean. *Deep Sea Research Part I: Oceanographic Research Papers*, *49*(9), 1623–1649. https://doi.org/10.1016/S0967-0637(02)00042-0

Mock, T., & Gradinger, R. (1999). Determination of Arctic ice algal production with a new in situ incubation technique. *Marine Ecology Progress Series*, *177*, 15–26. https://doi.org/10.3354/meps177015

Nakatsuka, T., Handa, N., Wada, E., & Wong, C. S. (1992). The dynamic changes of stable isotopic ratios of carbon and nitrogen in suspended and sedimented particulate organic matter during a phytoplankton bloom. *Journal of Marine Research*, *50*(2), 267–296. https://doi.org/10.1357/002224092784797692

Neeley, A. R., Harris, L. A., & Frey, K. E. (2018). Unraveling phytoplankton community dynamics in the Northern Chukchi sea under sea-ice-covered and sea-ice-free Conditions. *Geophysical Research Letters*, *45*(15), 7663–7671. https://doi.org/10.1029/2018GL077684

O'Daly, S. H., Danielson, S. L., Hardy, S. M., Hopcroft, R. R., Lalande, C., Stockwell, D. A., & McDonnell, A. M. P. (2020). Extraordinary carbon fluxes on the shallow Pacific Arctic shelf during a remarkably warm and low sea ice period. *Frontiers in Marine Science*, *7*, 986. https://doi.org/10.3389/fmars.2020.548931

Pelusi, A., Margiotta, F., Passarelli, A., Ferrante, M. I., d'Alcalà, M. R., & Montresor, M. (2020). Density-dependent mechanisms regulate spore formation in the diatom Chaetoceros socialis. *Limnology and Oceanography Letters*, *5*(5), 371–378. https://doi.org/10.1002/lol2.10159

Pitcher, G. C. (1990). Phytoplankton seed populations of the Cape Peninsula upwelling plume, with particular reference to resting spores of Chaetoceros (Bacillariophyceae) and their role in seeding upwelling waters. *Estuarine, Coastal and Shelf Science*, *31*(3), 283–301. https://doi.org/10.1016/0272-7714(90)90105-Z

Pomerleau, C., Nelson, R. J., Hunt, B. P. V., Sastri, A. R., & Williams, W. J. (2014). Spatial patterns in zooplankton communities and stable isotope ratios ($\delta^{13}C$ and $\delta^{15}N$) in relation to oceanographic conditions in the sub-Arctic Pacific and western Arctic regions during the summer of 2008. *Journal of Plankton Research*, *36*(3), 757–775. https://doi.org/10.1093/plankt/fbt129

Quinn, G. P., & Keough, M. J. (2002). *Experimental design and data analysis for biologists*. Cambridge University Press.

Sergeeva, V. M., Sukhanova, I. N., Flint, M. V., Pautova, L. A., Grebmeier, J. M., & Cooper, L. W. (2010). Phytoplankton community in the Western Arctic in July–August 2003. *Oceanology*, *50*(2), 184–197. https://doi.org/10.1134/S0001437010020049

Sherr, E. B., Sherr, B. F., & Hartz, A. J. (2009). Microzooplankton grazing impact in the Western Arctic Ocean. *Deep Sea Research Part II: Topical Studies in Oceanography*, *56*(17), 1264–1273. https://doi.org/10.1016/j.dsr2.2008.10.036

Smetacek, V. S. (1985). Role of sinking in diatom life-history cycles: Ecological, evolutionary and geological significance. *Marine Biology*, *84*(3), 239–251. https://doi.org/10.1007/BF00392493

Smith, W. O., Keene, N. K., & Comiso, J. C. (1988). Interannual Variability in Estimated Primary Productivity of the Antarctic Marginal Ice Zone. In D. Sahrhage (Ed.), *Antarctic ocean and resources variability* (pp. 131–139). Springer. https://doi.org/10.1007/978-3-642-73724-4_10

Springer, A. M., McROY, C. P., & Flint, M. V. (1996). The Bering Sea Green Belt: Shelf-edge processes and ecosystem production. *Fisheries Oceanography*, *5*(3–4), 205–223. https://doi.org/10.1111/j.1365-2419.1996.tb00118.x

Sugie, K., & Kuma, K. (2008). Resting spore formation in the marine diatom Thalassiosira nordenskioeldii under iron- and nitrogen-limited conditions. *Journal of Plankton Research*, *30*(11), 1245–1255. https://doi.org/10.1093/plankt/fbn080

Szymanski, A., & Gradinger, R. (2016). The diversity, abundance and fate of ice algae and phytoplankton in the Bering Sea. *Polar Biology*, *39*(2), 309–325. https://doi.org/10.1007/s00300-015-1783-z

Throndsen, J. (1978). The dilution-culture method. In A. Sournia (Ed.), *Phytoplankton manual* (pp. 218–224). Unesco.

Tsukazaki, C., Ishii, K.-I., Matsuno, K., Yamaguchi, A., & Imai, I. (2018). Distribution of viable resting stage cells of diatoms in sediments and water columns of the Chukchi Sea, Arctic Ocean. *Phycologia*, *57*(4), 440–452. https://doi.org/10.2216/16-108.1

Tsukazaki, C., Ishii, K.-I., Saito, R., Matsuno, K., Yamaguchi, A., & Imai, I. (2013). Distribution of viable diatom resting stage cells in bottom sediments of the eastern Bering Sea shelf. *Deep Sea Research Part II: Topical Studies in Oceanography*, *94*, 22–30. https://doi.org/10.1016/j.dsr2.2013.03.020

von Quillfeldt, C. H. (2000). Common diatom species in Arctic spring blooms: Their distribution and abundance. *Botanica Marina*, *43*(6), 499–516. https://doi.org/10.1515/BOT.2000.050

von Quillfeldt, C. H., Ambrose, W. G., & Clough, L. M. (2003). High number of diatom species in first-year ice from the Chukchi Sea. *Polar Biology*, *26*(12), 806–818. https://doi.org/10.1007/s00300-003-0549-1

Wang, S. W., Springer, A. M., Budge, S. M., Horstmann, L., Quakenbush, L. T., & Wooller, M. J. (2016). Carbon sources and trophic relationships of ice seals during recent environmental shifts in the Bering Sea. *Ecological Applications*, *26*(3), 830–845. https://doi.org/10.1890/14-2421

Werner, I., Ikävalko, J., & Schünemann, H. (2007). Sea-ice algae in Arctic pack ice during late winter. *Polar Biology*, *30*(11), 1493–1504. https://doi.org/10.1007/s00300-007-0310-2